Single-Fiber Bidirectional Filterless Metro Network

Filippo Cugini, Andrea Sgambelluri
CNIT
Pisa, Italy
filippo.cugini@cnit.it

Pantea Nadimi Goki, Francesco Paolucci, Marco Presi
Scuola Superiore Sant'Anna
Pisa, Italy
fr.paolucci@santannapisa.it

***Abstract*—Horseshoe filterless metro network is designed and experimentally validated for bidirectional transmission over a single fiber. Transmission impairments, dominated by in-band crosstalk, are specifically assessed, leading to extremely good transmission performance when misalignment in spectrum allocation is configured among the two directions.**

***Index Terms*—counter-propagation, scattering, full-duplex, drop and waste**

I. Introduction

Filterless solutions, originally proposed for low-cost core mesh implementations [1]–[3], have recently found remarkable interest for next generation metro networks based on horseshoe topology [4], see Fig. 1(a). In filterless networks, routers exploit coherent detection strategy while optical transport relies just on splitters/couplers and amplifiers, see Fig. 1(b), with no expensive Reconfigurable Optical Add/Drop Multiplexers (ROADM) and Wavelength Selective Switches (WSS).

As a major drawback, in filterless networks, a waste of spectrum resources is experienced since each signal occupies the entire network [5]–[10]. However, significant CAPEX and OPEX savings are expected due to the use of inexpensive hardware and thanks to the simple control and maintenance operations. To overcome the spectrum limitation and increase the overall capacity over the same infrastructure, recent studies have proposed dense wavelength deployments [11] and the cost-effective use of multi-band resources [12], also targeting edge-oriented scenario [13], along with SDN control plane extensions for disaggregated networks [14].

In this work, we propose and design a filterless metro network exploiting bidirectional transmission over a single fiber. Such solution is particularly attractive in case of limited fiber availability or in the cases where, due to regulatory aspects, network operators are forced to pay a rent to a government body/agency for any occupied fiber resources. Bidirectional single-fiber transmission has been extensively investigated in WDM Passive Optical Networks (WDM-PONs) where virtual point-to-point links use the same wavelength both for up- and down stream. Use of a single wavelength for bidirectional transmission is facilitated by the tree topology used in WDM-PONs, the presence of optical filters and the limited power budget, allowing for carrier or wavelength reuse schemes [15], [16]. The design of a filterless metro network exploiting bidirectional transmission over a single fiber has not been discussed yet.

II. Design of single-fiber filterless network

Fig. 1(b) shows a traditional filterless node exploiting two unidirectional fibers. The node encompasses EDFAs for signal re-amplification and splitter/couplers for channel add/drops. The evolution towards bidirectional inter-node single-fiber communication requires the introduction of optical circulators. Such components are low-cost passive devices typically providing less than 1dB attenuation on the clockwise direction and more than 40dB isolation on the counter-clockwise. This way, bidirectional transmission can take place on the fiber interconnecting two adjacent nodes while unidirectional transmission is experienced within the two branches of the node, thus enabling EDFAs to properly operate and safely perform add/drop onto the router interfaces.

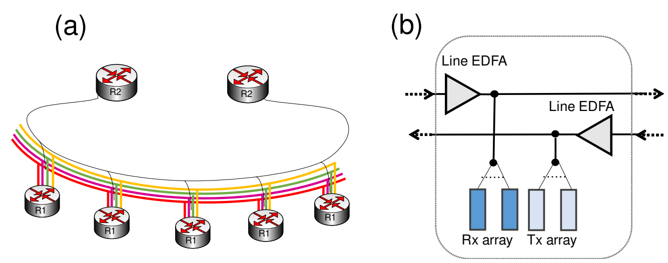

Fig. 1. Traditional filterless node exploiting two unidirectional fibers.

Three main aspects need to be taken into account in the dimensioning of the specific node characteristics when counter-propagation is experienced. First, amplifier gain has to be designed and configured sufficiently high to compensate span and component losses (i.e., splitter/coupler and circulators), but without introducing lasering effects in the potential loop between the two branches of the node. Second, optical reach has to account for the physical impairments due to counter-propagation experienced in the inter-node optical spans, i.e. Rayleigh scattering, which is responsible for reflecting both the optical signals and the ASE noise introduced by the amplifiers. Due to the presence of optical amplification, the impact of these reflections becomes important: at the network edges the impact of the reflections quadratically grows with the EDFA gain and the number of nodes. Third, spectrum assignment needs to be performed accounting for all sources of impairments and expected reach, possibly minimizing the impact of scattering effects and circulator crosstalk.

978-3-903176-21-8

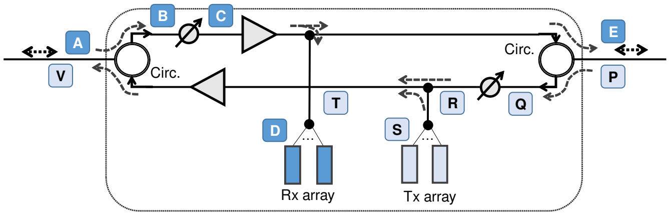

Fig. 2. Proposed filterless node for bidirectional single-fiber transmission.

Fig. 2 shows the proposed filterless node designed for bidirectional inter-node single-fiber communication. The target horseshoe metro network has up to N links, interconnecting the Central Office with N metro-access nodes. Metro-access nodes are designed to compensate for link lengths. Each node encompasses two circulators, and, for each direction, a variable optical attenuator, one EDFA and splitters/couplers. Among the possible interconnection options of these components, the design presented in Fig. 2 is here considered since it enables large flexibility in compensating various link lengths, even above 80km. Note that, in case of short link lengths, e.g. below 20-40 km depending on the receiver sensitivity, only one every two consecutive nodes can be equipped with EDFA. In this paper we focus on the former scenario of Fig. 2 since scattering effects are more detrimental compared to the latter case where re-amplification is not performed at every node.

III. Simulation Evaluation

The following metro parameters are first considered in the scheme of Fig. 2: $N = 10$ metro-access nodes, link length in typical metro range between $L_{MIN} = 10\,\text{km}$ and $L_{MAX} = 50\,\text{km}$ (even if the scheme would allow larger lengths), 1:2 in-line and at least 1:8 add/drop splitter/coupler (enabling interconnection of eight interfaces per node, but larger values can be considered), and EDFA gain of up to $G = 15\,\text{dB}$ (or larger) in the case of L_{MAX}. Optical launch power at the exit of each node is designed to be $P_E = P_V = 0\,\text{dBm}$ (points E and V in Fig. 2). The optical power entering the node (points A and O in Fig. 2) depends on the link length: for the considered cases, it remains in the range between $-10\,\text{dBm} \leq P_E = P_V \leq -2\,\text{dBm}$. Circulators are assumed with typical values of 1dB attenuation and 40dB isolation. The VOA in the upper $A - E$ direction is introduced in case of link lengths lower than L_{MAX}, such that the optical power entering the EDFA is fixed at $P_C = -11\,\text{dBm}$. Given the above EDFA gain, the optical power exiting the node is, as anticipated, $P_E = 0\,\text{dBm}$ while at the RX interface is $P_D = -8\,\text{dBm}$ (largely within the typical sensitivity values). In the lower $O - V$ direction, the VOA is configured, according to the link length, to fix the power $P_R = -11\,\text{dBm}$. This way, assuming a TX interface power of $P_S = -2\,\text{dBm}$, all express and added channels are equalized at $P_T = -14\,\text{dBm}$, leading to $P_V = 0\,\text{dBm}$. Interfaces are assumed at 100 Gb/s with PM-QPSK modulation format.

Fig. 3 shows the evolution of the in-band crosstalk effect due to the Rayleigh scattering in the case of L_{MAX} as a function of the traversed nodes, obtained by means of VPI simulation. Results show that the RX at the node 1 receives just a single scattering contribution, leading to less than -25dB reflected power. Instead, the signal generated at node 10 towards the central office is reamplified at each of the 10 traversed nodes, leading to 10 scattering contributions that cumulate at the RX of node 10 to a power value of around 15.4dB for link lengths of 50km.

TABLE I
Simulation results: expected OSNR and Xtalk levels for different link lengths

Link Length	OSNR (dB) 0.1nm	Signal/Xtalk Ratio (dB)
20	27.6	-22
30	27.2	-19.6
40	26.7	-17.4
50	26.4	-15.4

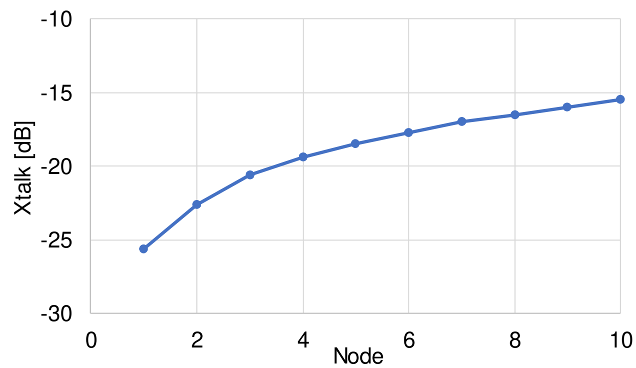

Fig. 3. In-band Crosstalk power as a function of the number of traversed nodes including Rayleigh scattering.

Table I shows the overall performance of the considered single-fiber bidirectional filterless network after 10 traversed nodes, considering different link lengths. Good OSNR performance is achieved, in the range between 26.4 and 27.6dB, with very limited sensitivity to link length. The dominating impairment is the in-band crosstalk, whose levels vary from 22dB for 20km links to the -15.4dB indicated above.

IV. Experimental validation

A portion of the considered horseshoe metro network is experimentally implemented. The testbed setup consists of two metro nodes emulating the transmission between the central office and the i-th node. Commercial interfaces at 100Gb/s PM-QPSK are considered. A link length of 25km is considered. To validate the scenario under different conditions, OSNR and crosstalk are varied to reproduce the simulation conditions. In particular, the in-band crosstalk is varied by introducing an additional independent 100Gb/s PM-QPSK signal at the same central frequency and with configurable power level.

Fig. 4 shows the experimental measurements of the Pre-FEC BER as a function of the in-band crosstalk. Measurements are collected at 27dB OSNR (noise loading implemented by

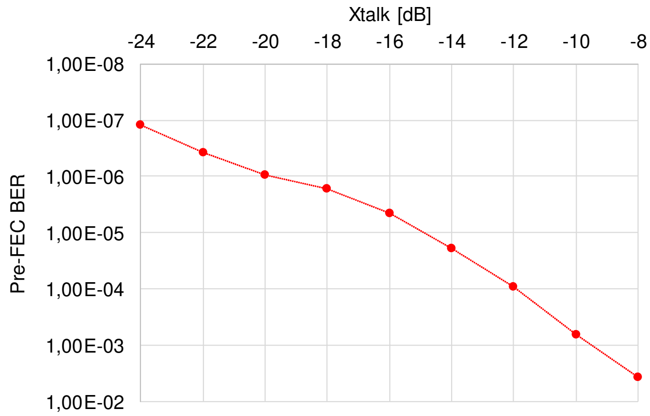

Fig. 4. Measured Pre-FEC BER at OSNR 27dB as a function of the in-band crosstalk.

using an open input EDFA), thus reproducing the conditions assessed through simulations and related to a horseshoe of 10 links. Results show that, at the expected worst case conditions indicated by the simulations, i.e. at 15.4dB signal-to-crosstalk ratio, the single-fiber bidirectional filterless network properly operates, experiencing a Pre-FEC BER safely around E-05. Large margin is experience since the system successfully operates until a crosstalk limit value of 8dB.

The measurements in Fig. 4 are performed assuming a nominal 50GHz spectrum assignment perfectly aligned between the two counter-propagating directions. However, by applying a shift of 25GHz between the two directions, the experienced crosstalk would be due only to back-scattered ASE noise, and therefore drastically reduced. Fig. 4 shows that in case of extremely limited or no relevant in-band crosstalk, the system operates at extremely good performance, i.e. with pre-FEC BER above E-06 after 10links of 50km.

V. Conclusions

This paper focused on the design and validation of horseshoe filterless metro network exploiting bidirectional transmission over a single fiber. Simulation analysis is conducted to assess the OSNR and Crosstalk performance achieved after 10 links of typical metro lengths (i.e. between 10 and 50km). Such conditions are experimentally reproduced using 100 Gb/s commercial coherent system. Results showed a safe 7dB operational margin when the same spectrum allocation is configured between the two directions. By then applying a 25GHz shift in one direction, extremely good performance is experienced. Thus, horseshoe filterless network exploiting bidirectional transmission over a single fiber represents an extremely attractive metro network solution also in consideration of the expected limited cost of the incoming generation of 100Gb/s PM-QPSK coherent pluggable modules.

Acknowledgment

This project has received funding from the ECSEL Joint Undertaking (JU) under grant agreement No 876967. The JU receives support from the European Union's H2020 research and innovation programme and from Italy Ministry of Education, University and Research (MIUR).

References

[1] C. Tremblay, F. Gagnon, B. Chatelain, E. Bernier, and M. Belanger, "Filterless optical networks : a unique and novel passive WAN network solution," in *12th OptoElectronic and Communications Conference (OECC)/ 16th International Conference on Integrated Optics and Optical Fiber Communication (OECC/IOOC'07)*, July 2007, pp. 12P–7.

[2] Z. Xu, E. Archambault, C. Tremblay, J. Chen, L. Wosinska, M. P. Belanger, and P. Littlewood, "1+1 dedicated optical-layer protection strategy for filterless optical networks," *IEEE communications letters*, vol. 18, no. 1, pp. 98–101, 2014.

[3] E. Archambault, N. Alloune, M. Furdek, Z. Xu, C. Tremblay, A. Muhammad, J. Chen, L. Wosinska, P. Littlewood, and M. P. Belanger, "Routing and spectrum assignment in elastic filterless optical networks," *IEEE/ACM Transactions on Networking*, vol. 24, no. 6, pp. 3578–3592, December 2016.

[4] B. Zaluski, B. Rajtar, H. Habjanic, M. Baranek, N. Slibar, R. Petracic, and T. Sukser, "Terastream implementation of all ip new architecture," in *2013 36th International Convention on Information and Communication Technology, Electronics and Microelectronics (MIPRO)*, May 2013, pp. 437–440.

[5] O. Ayoub, S. Shehata, F. Musumeci, and M. Tornatore, "Filterless and semi-filterless solutions in a metro-haul network architecture," in *2018 20th International Conference on Transparent Optical Networks (ICTON)*, July 2018, pp. 1–4.

[6] B. Jaumard, Y. Wang, and N. Huin, "Optimal design of filterless optical networks," in *2018 20th International Conference on Transparent Optical Networks (ICTON)*, July 2018, pp. 1–5.

[7] B. Shariati, M. Ruiz, A. Sgambelluri, F. Cugini, and L. Velasco, "Real-time spectrum surveillance in filterless optical networks," in *2018 Optical Fiber Communications Conference and Exposition (OFC)*, March 2018, pp. 1–3.

[8] F. Cugini, C. Porzi, N. Sambo, A. Bogoni, and P. Castoldi, "Receiver architecture with filter for power-efficient drop waste networks," in *2016 Optical Fiber Communications Conference and Exhibition (OFC)*, March 2016, pp. 1–3.

[9] C. Tremblay, P. Littlewood, M. P. Bélanger, L. Wosinska, and J. Chen, "Agile filterless optical networking," in *2017 International Conference on Optical Network Design and Modeling (ONDM)*, May 2017, pp. 1–4.

[10] M. Furdek, A. Muhammad, G. Zervas, C. Tremblay, and L. Wosinska, "Performance evaluation of programmable filterless networks implemented by optical white boxes," in *2016 18th International Conference on Transparent Optical Networks (ICTON)*, July 2016, pp. 1–1.

[11] D. Uzunidis, E. Kosmatos, C. Matrakidis, A. Stavdas, and A. Lord, "DuFiNet: Architectural considerations and physical layer studies of an agile and cost-effective metropolitan area network," *Journal of Lightwave Technology*, vol. 37, no. 3, pp. 808–814, Feb 2019.

[12] F. Paolucci, R. Emmerich, F. Fresi, I. Sackey, L. Poti, C. Schubert, J. Fischer, and F. Cugini, "Filterless optical WDM metro networks exploiting C+L band," in *2018 European Conference on Optical Communications (ECOC 2018)*, Sept 2018.

[13] F. Paolucci, R. Emmerich, A. Eira, N. Costa, J. Pedro, P. W. Berenguer, C. Schubert, J. K. Fischer, F. Fresi, A. Sgambelluri, and F. Cugini, "Disaggregated edge-enabled C+L-band filterless metro networks," *IEEE/OSA Journal of Optical Communications and Networking*, vol. 12, no. 3, pp. 2–12, March 2020.

[14] F. Paolucci, A. Sgambelluri, R. Emmerich, A. Giorgetti, P. Castoldi, C. Schubert, J. Fischer, and F. Cugini, "OpenConfig control of 100G/400G filterless metro networks with configurable modulation format and FEC," in *Optical Fiber Communication Conference (OFC) 2019*. Optical Society of America, 2019, p. Tu3H.4.

[15] M. Presi, M. Rannello, M. Artiglia, I. Tomkos, I. Cano, J. Prat, and E. Ciaramella, "Hitless wavelength assignment in filterless optical access networks," in *2016 18th International Conference on Transparent Optical Networks (ICTON)*, July 2016, pp. 1–4.

[16] J. A. Lazaro, C. Arellano, V. Polo, and J. Prat, "Rayleigh scattering reduction by means of optical frequency dithering in passive optical networks with remotely seeded onus," *IEEE Photonics Technology Letters*, vol. 19, no. 2, pp. 64–66, Jan 2007.